

DanceMeld: Unraveling Dance Phrases with Hierarchical Latent Codes for Music-to-Dance Synthesis

Xin Gao, Li Hu, Peng Zhang, Bang Zhang, Liefeng Bo
Institute for Intelligent Computing, Alibaba Group

{zimu.gx, hooks.hl, futian.zp, zhangbang.zb, liefeng.bo}@alibaba-inc.com

<https://humanaigc.github.io/dance-meld/>

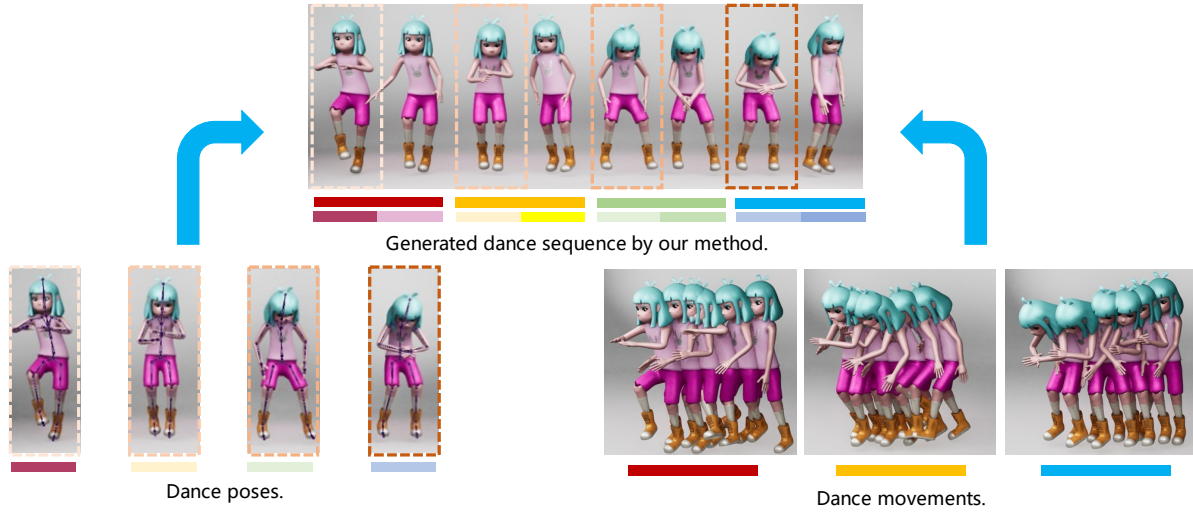


Figure 1. In the field of choreography, dance poses composed of a series of basic meaningful body postures, while dance movements can reflect trends, rhythm and energy of the motion. Our method uses a hierarchical VQ-VAE to decouple dance poses and dance movements by representing them with bottom code and top code (short line for bottom code and long line for top code).

Abstract

In the realm of 3D digital human applications, music-to-dance presents a challenging task. Given the one-to-many relationship between music and dance, previous methods have been limited in their approach, relying solely on matching and generating corresponding dance movements based on music rhythm. In the professional field of choreography, a dance phrase consists of several dance poses and dance movements. Dance poses composed of a series of basic meaningful body postures, while dance movements can reflect dynamic changes such as the rhythm, melody, and style of dance. Taking inspiration from these concepts, we introduce an innovative dance generation pipeline called DanceMeld, which comprising two stages, i.e., the dance decouple stage and the dance generation stage. In the decouple stage, a hierarchical VQ-VAE is used to disentangle dance poses and dance movements in different feature space

levels, where the bottom code represents dance poses, and the top code represents dance movements. In the generation stage, we utilize a diffusion model as a prior to model the distribution and generate latent codes conditioned on music features. We have experimentally demonstrated the representational capabilities of top code and bottom code, enabling the explicit decoupling expression of dance poses and dance movements. This disentanglement not only provides control over motion details, styles, and rhythm but also facilitates applications such as dance style transfer and dance unit editing. Our approach has undergone qualitative and quantitative experiments on the AIST++ dataset, demonstrating its superiority over other methods.

1. Introduction

Virtual characters have been popular in various domains, including virtual idols, virtual customer service, and vir-

tual assistants. Driving virtual characters to dance with music is an important application within the gaming industry, film production and AR/VR experiences. However, creating dance animations demands professional expertise to match intricate movements with diverse music styles, rhythm, and melodies. As a result, automated dance generation holds substantial promise, offering a straightforward and cost-effective means for individuals to produce and edit dance sequences for 3D characters, reducing the need for extensive manual effort during the production process. Music-driven dance generation remains an ongoing research challenge owing to the intricate one-to-many relationships that exist between music and dance. Recent studies have aimed to address this challenge using machine learning techniques such as Generative Adversarial Networks (GANs) [20, 22], autoregressive models [14, 17, 22, 23, 35, 41], and diffusion models [1, 6, 24, 38]. Unfortunately, most previous music-to-dance methods treat the task as a general human motion generation task, mapping frame-level dance motion directly to sequential music, without taking choreography knowledge into account.

To tackle this issue, we refer to expert knowledge of professional choreography [3, 28]. Dance phrase, which expresses the complete meaning of a smallest dance sequence, serves as the basic unit in choreography. To create a dance phrase, the choreographer should: 1) conceive several meaningful dance poses, 2) connect these dance poses with appropriate dance movements in terms of space, shape, time, energy and emotion from music. Therefore, dance poses and dance movements are two key elements in professional choreography. Despite drawing inspiration from the knowledge mentioned above, it is still challenge to model dance poses and dance movements. In real dance motions, poses and movements do not exhibit a straightforward one-to-one mapping, they are intricately intertwined, which represent artistic combinations that are influenced by the dance genre, style, and the rhythm and melody of the music, making it difficult to disentangle. Recently, Bailando [33] proposes to establish a dancing pose unit dictionary to learn a dancing-style subspace. However, it still needs an extra actor-critic learning with a reward function to align between motion tempo and music beats.

In this paper, we introduce a novel dance generation pipeline called DanceMeld that comprising two stages: the dance decouple stage and the dance generation stage. In the dance decouple stage, inspired by previous works in text-to-image synthesis, we employ a hierarchical Vector Quantized Variational Autoencoder (VQ-VAE) [31, 39] to model dance poses and dance movements separately in different feature space levels, where the bottom latent code aims to indicate a certain reasonable dance poses, and the top latent code energizes the representation of movement process which capturing aspects such as orientation, tendency,

speed and beat of the motion. In the dance generation stage, we leverage a diffusion model as a prior to generate the sequence of latent codes based on the given music. These predicted code sequences are decoded into dance sequences using a motion decoder. In summary, our contributions are as follows:

- We propose DanceMeld, a two-stage music-to-dance framework that decouple dance poses and dance movements by representing them with bottom code and top code by a hierarchical VQ-VAE, experiments demonstrate the interpretability of the latent codes.
- A diffusion model is used as a prior to represent the distribution of latent codes and generate dance sequences conditioned on music, which enables various applications such as dance style transfer and dance unit editing.
- Our approach has been validated both qualitatively and quantitatively on the AIST++ dataset compared to the state-of-the-art methods, demonstrating its effectiveness and superiority.

2. Related Works

2.1. Music-to-Dance

Music-to-dance is a sub-task within Human Motion Synthesis: the generation of human body movements that align with the characteristics of the music, such as its genre, rhythm, and intensity. A classic approach involves using Graph-based Motion Synthesis methods [4, 10], which segment the motions in the dataset into various nodes. Edges between nodes are added based on their similarity. When provided with input music, this task can be regarded as a retrieval task, where the corresponding motion nodes are selected by matching the speed and amplitude of character movements in motion segments to the rhythm and intensity of the music. However, Graph-based methods have their limitations, this cutting-and-pasting approach lacks diversity. To address this issue, [48] uses auto-regressive generative model to generate 3D dance motions with high realism and diversity, [22, 23, 29, 35, 42] use transformer-based architecture to generate more diversified dance motion that are well-attuned to the input music. However, auto-regressive models suffer from the issue of error accumulation, making it prone to freezing when generating long sequences of dance motions. [2] try to generate long-term sequences of human motions by forming a global structure that respects a specific dance genre. [14] proposes a curriculum learning strategy to alleviate error accumulation of auto-regressive models in long motion sequence generation.

Human choreographers design dance motions from music by firstly devising multiple choreographic dance units and then arranging the dance unit sequence according to music’s rhythm, melody and emotion [3, 28]. Inspired by this, [20, 41] decompose a dance sequence into a series of

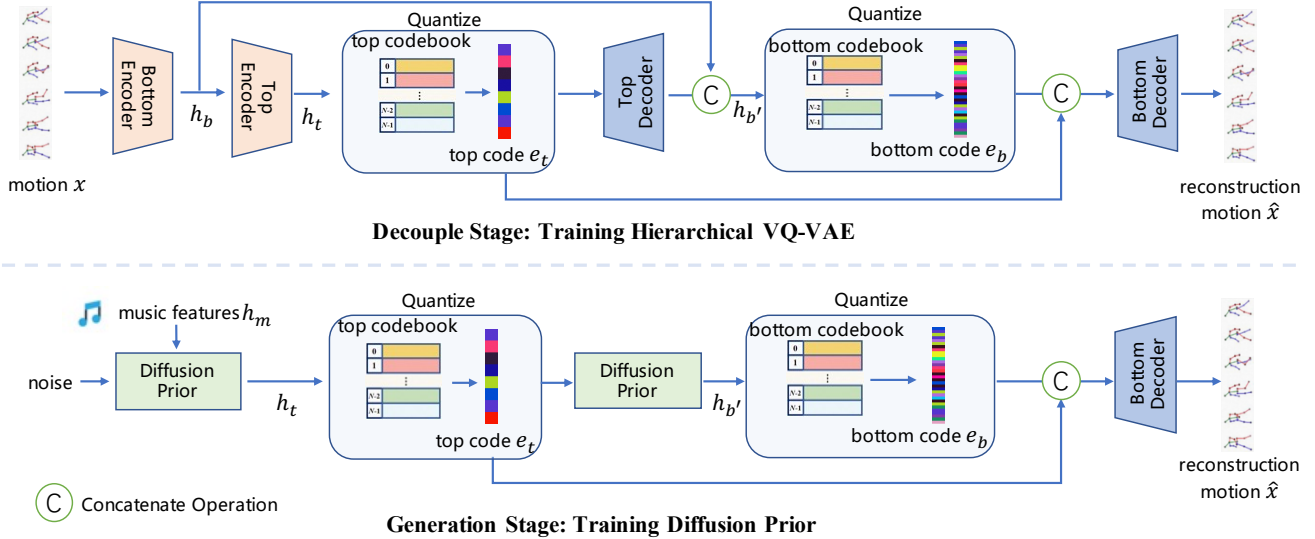


Figure 2. Our method comprises two stages: the dance decouple stage and the dance generation stage. In the dance decouple stage, a hierarchical VQ-VAE is trained to decouple dance pose and dance movement by representing them with bottom code e_b and top code e_t . In the motion generation phase, a diffusion model is employed as a prior to model the distribution of latent codes. The latent codes are then decoded into dance sequences by a motion decoder.

basic dance units and then compose a dance by organizing multiple basic dancing movements seamlessly according to the input music. [33] utilizes VQ-VAE to encode and quantize 3D pose sequences and then employs a transformer based architecture to combine these discrete codes and generate corresponding motions.

2.2. Motion Diffusion Models

Human motion generation, learned from motion capture data, can be conditioned by any signal that describes the motion, such as text and audio. For the text-to-motion task, [13, 36] represent motions as images and utilize the CLIP model [30] to align texts and images in latent space, enabling texts to control the generation of motions. The success of generative models in the text-to-image task has spurred the exploration of diffusion-based models in motion generation task. [5, 18, 37, 43–45] employ diffusion models to address the text-to-motion task, while [38, 46] use diffusion models to tackle the music-to-dance task. Given that text, audio, and music all serve as conditions for motion generation task, [6, 11, 27, 47] address these sub-tasks simultaneously by designing a unified generative framework. One of the challenges in motion generation is the problem of generating long sequences. [38] generates choreographies of any length by imposing temporal constraints on batches of sequences. [32] generates arbitrarily-long sequences with text control per interval using a fixed motion diffusion prior. [21] generates long-term 3D human motion from multiple action labels.

2.3. Hierarchical VQ-VAE

VQ-VAE [39] is a generative model that leverages vector quantization to efficiently encode and decode high-dimensional data. The encoder learns a discrete latent representation, and the auto-regressive decoder is learnt as a prior to generate images. To obtain higher-quality images, generative models often employ the coarse to fine strategy to generate images progressively. For example, StyleGAN [15, 16] uses a synthesis network to progressively increase the feature resolutions and recovering high-resolution images from sampled noise. [7, 31] introduce a hierarchical VQ-VAE structure comprising multiple nested encoders and decoders. In the field of music generation, [8, 9] also utilize the hierarchical VQ-VAE to represent more abstract musical features. A key feature of this kind of model is its use of multiple discrete codebooks during the encoding and decoding processes. The lower-level codebook captures fine-grained details, while the top-level codebook captures higher-level semantic information.

3. Method

3.1. Overview

In the professional field of choreography, a dance phrase consists of several dance poses and dance movements. Dance poses composed of a series of basic meaningful body postures, while dance movements can reflect dynamic changes such as the rhythm, melody, and style of dance. Despite drawing inspiration from the knowledge mentioned

above, it is still a challenge to model dance poses and dance movements. In real dance motions, poses and movements do not exhibit a straightforward one-to-one mapping, they are intricately intertwined and difficult to disentangle. We try to decouple and represent dance poses and dance movements explicitly by carefully selecting appropriate model structures and designing loss functions.

In Sec.3.3, a hierarchical VQ-VAE architecture is used to disentangle and model dance poses and dance movements in different feature space levels, with the bottom latent code representing dance poses and the top latent code representing dance movements. The relevant experiments in Sec.4.3 demonstrated the interpretability of latent codes. In Sec.3.4, we design a prior for modeling and sampling the latent codes of dance poses and dance movements by using a diffusion model. Music features are incorporated as conditions, ensuring that the generated dance motions match the music’s type, rhythm, and intensity. The latent codes are fed into a decoder to reconstruct the dance motion sequence.

3.2. Data Representation

Dance motions are represented by sequences of 3D human joints based on the SMPL model [25], which includes root’s global positions and 6D rotation representation of 24 joints, resulting in a total dimension of $\mathbf{x} \in \mathbb{R}^{N \times w}$, where $w \in \mathbb{R}^{3+24*6=147}$ is the dimension of motion features and N is the sequence number of frames. The music features \mathbf{h}_m are extracted from the jukebox encoder [8], which is a large generative model trained on 1M songs and the features should have good representational ability for different types of music.

3.3. Hierarchical VQ-VAE

The hierarchical VQ-VAE structure comprising multiple nested encoders and decoders. The lower-level features capture fine-grained details, while the top-level features capture higher-level semantic information. For motion, its semantic manifestation occurs in the temporal domain. Short-term motion represents specific postures, while the continuous variation of motion over a longer duration can reflect the semantic information. We use the hierarchical VQ-VAE and extract representations from intermediate layers to represent dance poses and dance movements. During the encoding process, the dimension of features gradually increases to express more abstract characteristics. The temporal dimension compresses, enabling the representation of a broader temporal range. Therefore, the low-level latent codes are used to represent dance poses, while the top-level latent codes are employed to represent dance movements.

Specifically, the motion input \mathbf{x} passes through encoders \mathbf{E}_b and \mathbf{E}_t to obtain bottom feature \mathbf{h}_b and top feature \mathbf{h}_t , respectively. The top code \mathbf{e}_t is obtained by the *Quantize*

operation [39], which are quantized vectors based on their distances to the prototype vectors in the codebook. Similarly, the bottom code \mathbf{e}_b is the quantized results of \mathbf{h}'_b , where \mathbf{h}'_b is the concatenate results of \mathbf{h}_b and the result after passing through decoder \mathbf{D}_t for \mathbf{e}_t . \mathbf{e}_b and \mathbf{e}_t are then concatenated and fed into the decoder \mathbf{D}_b to get the reconstructed result $\hat{\mathbf{x}}$:

$$\mathbf{h}_b = \mathbf{E}_b(\mathbf{x}), \mathbf{h}_t = \mathbf{E}_t(\mathbf{h}_b) \quad (1)$$

$$\mathbf{e}_t = \text{Quantize}(\mathbf{h}_t), \mathbf{h}'_b = \text{Concat}(\mathbf{D}_t(\mathbf{e}_t), \mathbf{h}_b) \quad (2)$$

$$\mathbf{e}_b = \text{Quantize}(\mathbf{h}'_b), \hat{\mathbf{x}} = \mathbf{D}_b(\text{Concat}(\mathbf{e}_t, \mathbf{e}_b)) \quad (3)$$

The whole pipeline is shown in Fig.2. For training the hierarchical VQ-VAE, the reconstruction loss with the commit losses are employed:

$$\begin{aligned} \mathcal{L}_{VQ}(\mathbf{x}, \hat{\mathbf{x}}) = & \|sg[\mathbf{h}'_b] - \mathbf{e}_b\|_2^2 + \alpha \|sg[\mathbf{e}_b] - \mathbf{h}'_b\|_2^2 \\ & + \|sg[\mathbf{h}_t] - \mathbf{e}_t\|_2^2 + \beta \|sg[\mathbf{e}_t] - \mathbf{h}_t\|_2^2 + \|\mathbf{x} - \hat{\mathbf{x}}\|_2^2 \end{aligned} \quad (4)$$

In addition to using L_2 loss for motion reconstruction to train encoders, the corresponding codebooks for the two VQ-VAE networks are also trained simultaneously. And two commit losses are used to ensure that the embedding results of the encoders do not grow. Here the operator *sg* refers to the stop-gradient operation that blocks gradients from flowing into its argument.

To improve physical realism in the absence of true simulation, we use four auxiliary losses: joint positions (Eq.5), velocities (Eq.6), accelerates (Eq.7) and contact (Eq.8) losses:

$$\mathcal{L}_{pos} = \|\mathbf{FK}(\mathbf{x}) - \mathbf{FK}(\hat{\mathbf{x}})\|_2^2 \quad (5)$$

$$\mathcal{L}_{vel} = \frac{1}{N-1} \sum_{i=1}^{N-1} \|(\mathbf{x}^{i+1} - \mathbf{x}^i) - (\hat{\mathbf{x}}^{i+1} - \hat{\mathbf{x}}^i)\|_2^2 \quad (6)$$

$$\mathcal{L}_{acc} = \frac{1}{N-1} \sum_{i=1}^{N-1} \|(\mathbf{v}^{i+1} - \mathbf{v}^i) - (\hat{\mathbf{v}}^{i+1} - \hat{\mathbf{v}}^i)\|_2^2 \quad (7)$$

$$\mathcal{L}_{contact} = \frac{1}{N-1} \sum_{i=1}^{N-1} \|(\mathbf{FK}(\hat{\mathbf{x}}^{i+1}) - \mathbf{FK}(\hat{\mathbf{x}}^i)) \cdot \mathbf{b}^i\|_2^2 \quad (8)$$

where $\mathbf{FK}(\cdot)$ denotes the forward kinematic function which converts joint angles into joint positions, $\mathbf{v} = \mathbf{x}^{i+1} - \mathbf{x}^i$, and \mathbf{b}_i is the binary foot contact label of the pose at each frame i . The overall auxiliary loss is as follows:

$$\mathcal{L}_{aux} = \mathcal{L}_{pos} + \gamma \mathcal{L}_{vel} + \phi \mathcal{L}_{acc} + \psi \mathcal{L}_{contact} \quad (9)$$

In addition, we also use a modality alignment loss \mathcal{L}_{MA} to align top code \mathbf{e}_t which represents dance movements to high-level music features \mathbf{h}_m :

$$\mathcal{L}_{MA} = \|\mathbf{e}_t - \mathbf{h}_m\|_2^2 \quad (10)$$

Final training loss is the weighted sum of the above losses:

$$\mathcal{L} = \mathcal{L}_{VQ} + \lambda_{aux}\mathcal{L}_{aux} + \lambda_{MA}\mathcal{L}_{MA} \quad (11)$$

3.4. Diffusion Model as Prior

The next step is to learn a prior over the latent codes, thus motions can be generated from sampled latent codes conditioned with music features. Recently, the success of generative models in the text-to-image task has spurred the exploration of diffusion-based models in motion generation task. Diffusion models can learn the distribution of the latent space, aligning similar textual or music conditions with corresponding similar motion sequences. In addition to this, it has advantages in long-term dependency modeling and exhibits superior generation diversity. Based on the above analysis of its advantages, we consider the transform based diffusion model as the prior. Two choices can be chosen, whether to use VQ-Diffusion [12] to model the distribution of the discrete latent codes $p(\mathbf{e}_b, \mathbf{e}_t | \mathbf{h}_m)$, or use traditional gaussian diffusion to model the distribution of the continuous latent features $p(\mathbf{h}'_b, \mathbf{h}_t | \mathbf{h}_m)$ while preserving the codebooks. We've tried both and opt for the latter because it yields better results.

For the conditional joint probability distribution $p(\mathbf{h}'_b, \mathbf{h}_t | \mathbf{h}_m)$, it can be further expressed as $p(\mathbf{h}_t | \mathbf{h}_m)p(\mathbf{h}'_b | \mathbf{h}_t, \mathbf{h}_m)$. Therefore, we can use two diffusion models to separately model the conditional distribution $p(\mathbf{h}_t | \mathbf{h}_m)$ and $p(\mathbf{h}'_b | \mathbf{h}_t, \mathbf{h}_m)$, as shown in Fig.3(a). Another approach is to directly predict the joint probability distribution $p(\mathbf{h}'_b, \mathbf{h}_t | \mathbf{h}_m)$ by concatenating \mathbf{h}_t and \mathbf{h}'_b , and then using a single diffusion model to model the joint probability distribution, as shown in Fig.3(b). For detailed comparative experiments and results, please refer to Sec.4.2. Here we choose the latter for better clarification. We jointly model \mathbf{h}'_b and \mathbf{h}_t by concatenating them: $\mathbf{h} = \text{Concat}(\mathbf{h}'_b, \mathbf{h}_t)$, and follow the DDPM definition of diffusion as a Markov noising process, $\{\mathbf{h}^{(t)}\}_{t=0}^T$, where $\mathbf{h}^{(0)}$ is drawn from the data distribution and the forward process is defined as:

$$q(\mathbf{h}^{(t)} | \mathbf{h}^{(t-1)}) \sim \mathcal{N}(\sqrt{1 - \beta_t}\mathbf{h}^{(t-1)}, \beta_t \mathbf{I}) \quad (12)$$

where $\beta_t \in (0, 1)$ and \mathbf{I} is the standard normal distribution. To approximate the distribution $p(\mathbf{h}^{(0)} | \mathbf{h}_m)$, a transformer based neural network \mathbf{G} is used to parameterize the chained reverse diffusion process $p_{\mathbf{G}}(\mathbf{h}^{(t-1)} | \mathbf{h}^{(t)}, \mathbf{h}_m)$ by directly predicting the clean sequence $\mathbf{h}^{(0)}$ as $\hat{\mathbf{h}}^{(0)} = \mathbf{G}(\mathbf{h}^{(t)}, t, \mathbf{h}_m)$. The generator \mathbf{G} is optimized by the L_2 loss:

$$\mathcal{L} = \mathbb{E}_{\mathbf{h}^{(0)}, t} [\|\mathbf{h}^{(0)} - \hat{\mathbf{h}}^{(0)}\|_2^2] \quad (13)$$

In the inference stage, given the extracted music feature \mathbf{h}_m as condition, we use DDIM to sample and gradually denoise $\mathbf{h}^{(t)}$ from noise, for timestep $t - 1$: $\hat{\mathbf{h}}^{(t-1)} \sim$

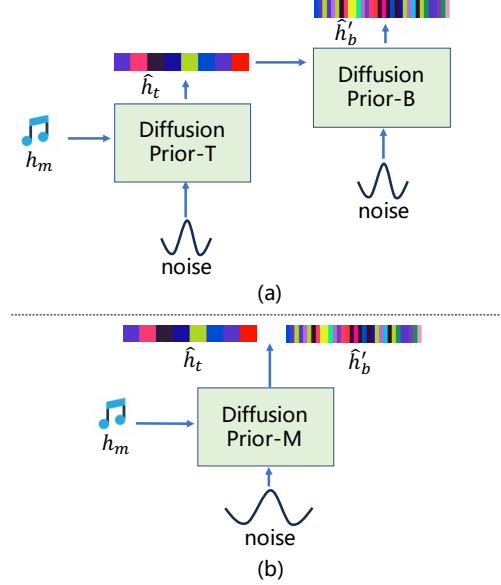


Figure 3. Different prior model arthitecture. (a) Separatel model $p(\mathbf{h}_t | \mathbf{h}_m)$ and $p(\mathbf{h}'_b | \mathbf{h}_t, \mathbf{h}_m)$. (b) Predict the joint probability $p(\mathbf{h}_b, \mathbf{h}_t | \mathbf{h}_m)$ by concatenating \mathbf{h}_t and \mathbf{h}'_b .

$q(\mathbf{G}(\mathbf{h}^{(t)}, t, \mathbf{h}_m), t - 1)$. After predicting $\hat{\mathbf{h}}^{(0)}$, the final motion sequence can be obtained by the motion decoder.

4. Experiments

Dataset. We perform the training and evaluation on AIST++ dataset [23], which consists of 1,408 sequences of 3D human dance motion and are paired to music. The durations vary from 7.4 sec. to 48.0 sec. We re-use the train/test splits provided by the original dataset.

Implementation details. We conduct pre-processing to segment the dance sequence to 512, the FPS is set at 60, the sliding window is 40. We use the features from the 36th layer of the Jukebox encoder, and a small encoder is employed to reduce the feature dimension to align with the top code. Same as motion input, the music feature's frame rate is also set at 60 FPS. We employed a hierachical VQ-VAE with a total of 54M parameters. The downsample rate of the bottom encoder \mathbf{E}_b and the top encoder \mathbf{E}_t is 4 and 2, respectively. The dictionary size of the bottom codebook is set to 512, and 128 for the top codebook. The feature dimensions for both bottom code and top code is set to 512. The hyperparameters $\alpha = \beta = 0.02$, $\gamma = \phi = \psi = 1$, $\lambda_{aux} = 1$, $\lambda_{MA} = 0.1$. Adam Optimizer [19] is used with $lr = 1e^{-4}$. The network is trained for 1000 epochs with a batch size of 64. The diffusion process is implemented using DDPM with 1000 steps, by directly predicting $\mathbf{h}^{(0)}$ with a transformer encoder. The encoder has 8 layers, 8

Methods	Motion Quality		Motion Diversity		Beat Align.↑	PFC↓	User Study	
	FID _k ↓	FID _g ↓	Div _k →	Div _g →			Ours	WinRate
Ground Truth	17.10	10.60	9.48	7.32	0.24	1.33	58.8%	
FACT [23]	35.35	22.11	5.94	6.18	0.22	2.25	92.5%	
Bailando [33]	28.16	9.62	7.83	6.34	0.23	1.75	86.3%	
EDGE [38]	-	-	10.68	7.62	0.27	1.65	64.6%	
DanceMeld (Ours)	22.74	9.18	8.74	7.89	0.28	1.72	N/A	

Table 1. Numerical metrics of FACT [23], Bailando [33], EDGE [38], and our method on AIST++ dataset. ↓ indicates lower is better, → indicates closer to ground truth is better. Our method outperforms other approaches in terms of generated quality, as evidenced by the FID metric and validated by the User Study. In terms of diversity, our method remains on par with EDGE. Due to the incorporation of modality alignment loss and auxiliary losses, our method also exhibits advantages in terms of aligning with the beat of the music and PFC metrics.

attention heads, and a latent dimension of 512. For training the transformer encoder, a learning rate of $4e^{-4}$ is used with the Adan optimizer [40] over 500 epochs. More details please refer to the supplementary materials.

4.1. Comparison to Existing Methods

We compare our method against three state-of-the-art approaches: FACT [23], Bailando [33], and EDGE [38]. For evaluate metrics, we first extract kinetic feature and geometric feature, following the same steps as in [23]. We evaluate the generated motion quality by calculating the distribution distance between the generated and the ground-truth motions using Fréchet Inception Distance (FID) on the extracted kinetic feature and geometric feature, FID_k and FID_g, respectively. For the motion diversity, we calculate the average Euclidean distance in the feature space across 40 generated motions on the AIST++ test set. The motion diversity in the geometric feature space and in the kinetic feature space are noted as Div_k, Div_g, respectively. In addition, we also use Beat Alignment Score (BAS) [23] to characterize the alignment between the dance motions and the musical rhythm. The Physical Foot Contact (PFC) score [38] is also introduced to evaluate physical plausibility. Just as discussed in [38], due to the lack of a proficient motion encoder to represent the motion features, the FID metrics maybe unreliable as a measure of quality on this dataset. Thus human evaluations are introduced as a supplementary measure to qualitatively evaluate from a visual perspective. We hired 20 participants on an outsourcing platform for the User Study. We randomly selected 100 segments, each lasting 10 seconds, and had each participant make judgments. Each sample had results from our method and a randomly selected comparison method (including ground truth), both generated using the same music. Participants were asked to determine which dance result exhibited better generation quality and better alignment with the music.

The quantitative results are as shown in Tab. 1. Quantitatively, our method outperforms other approaches in terms of generated quality, as evidenced by the FID metric and validated by the User Study. In terms of diversity, our method

Methods	Motion Quality		Motion Diversity	
	FID _k ↓	FID _g ↓	Div _k →	Div _g →
Ours (Best)	22.74	9.18	8.74	7.89
VQ-Diffusion	35.35	22.11	5.94	6.18
Single VQ-VAE	25.48	11.75	7.96	6.12
Prior-B+T	28.16	9.62	7.83	6.34

Table 2. Ablation study on different network architectures. VQ-Diffusion predicts discrete latent codes distribution $p(e_b, e_t | \mathbf{h}_m)$. Single VQ-VAE means not use hierarchical VQ-VAE. Prior-B+T refers to the architecture that use two diffusion models.

remains on par with EDGE, which also relies on diffusion-based sampling. Due to the incorporation of modality alignment loss and auxiliary losses, our method also exhibits advantages in terms of aligning with the rhythm of the music and maintaining the authenticity of footstep movements.

4.2. Ablation Studies

Network Selection. We conduct relevant ablation studies on the selection and design of network structures. Our optimal model utilizes a hierarchical VQ-VAE architecture, employing the traditional gaussian diffusion to directly predict the joint probability distribution $p(\mathbf{h}'_b, \mathbf{h}_t | \mathbf{h}_m)$. When using VQ-Diffusion to predict the discrete probability distribution $p(e_b, e_t | \mathbf{h}_m)$, we observed a significant decrease in the metrics. We suspect that the mask-and-replace diffusion strategy on VQ-Diffusion still has some limitations compared to gaussian diffusion process. Next, we replace the hierarchical VQ-VAE model with a single VQ-VAE model and also observed some decrease in the metrics. Our third comparative experiment involves using two diffusion models to predict conditional probability distributions for $p(\mathbf{h}_t | \mathbf{h}_m)$ and $p(\mathbf{h}'_b | \mathbf{h}_t, \mathbf{h}_m)$, as shown in Fig.3(b), the results were slightly inferior compared to directly predicting the joint probability distribution. The corresponding results are shown in Tab. 2.

Methods	Motion Quality		Beat Align.↑	PFC↓
	FID _k ↓	FID _g ↓		
Baseline	22.74	9.18	0.28	1.72
w/o \mathcal{L}_{aux}	21.40	13.63	0.27	2.16
w/o \mathcal{L}_{MA}	27.90	8.91	0.23	1.84

Table 3. The ablation study result of loss terms. The use of \mathcal{L}_{aux} can improve physical realism and enhance temporal stability. The use of \mathcal{L}_{MA} improves the BAS metric.

Loss Terms. Here we discuss the impact of each loss term on the generated results. As seen in Tab.3, when auxiliary losses are not used, the PFC metric significantly deteriorates. Although FID_k shows a slight improvement, the generated motions exhibit minor fluctuations between time steps. These results suggest that contact loss may contribute to maintaining the authenticity of footstep movements, and the velocity and acceleration losses in the auxiliary losses contribute to temporal stability.

The introduction of modality alignment loss enables the alignment of motion’s top code and music features in the high-level latent space, allowing the top code to better represent music-related features, such as rhythm and melody. From Tab.3, it can be observed that when modality alignment loss is not used, the BAS metric significantly decreases. Additionally, we randomly selected some in the wild music and extracted beat information from both music and motion. The visual results in Fig.4 intuitively demonstrate that the modality alignment loss enhances the alignment of music and motion in terms of rhythm.

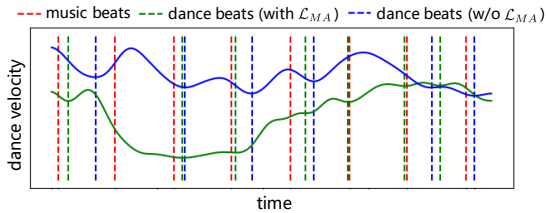


Figure 4. After using modality alignment loss, beats between dance motions and music are more synchronized.

4.3. The Interpretability of Latent Codes

In our approach, bottom code can be explicitly represented as dance poses, while top code can characterize more abstract dance movements. We will validate the representational capabilities of the bottom code and top code through several visual experiments.

The Interpretability of Bottom Code. We design the following experiment to validate that bottom code can represent dance poses. By fixing the bottom code and changing

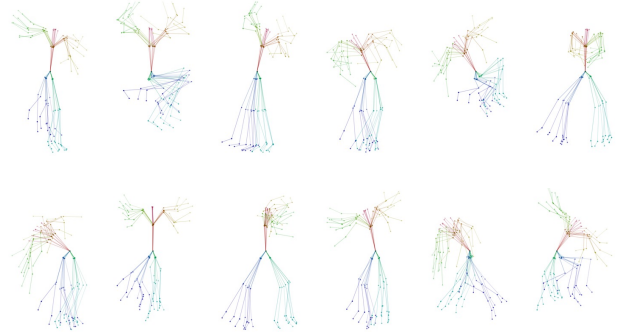


Figure 5. We present dance poses for 12 distinct bottom codes, combining each with a random selection of several top codes for visualization. The results reveal that the poses are constrained within a fixed range.

the top code, we found that the generated motions were restrained within a fixed range. Fig.5 shows 12 examples, each example represents the overlapped visual results of a fixed bottom code with different top codes. It is evident that the poses are restrained within a certain range. Different bottom codes correspond to different dance poses with clear distinctions. More visual results please refer to the supplementary materials.

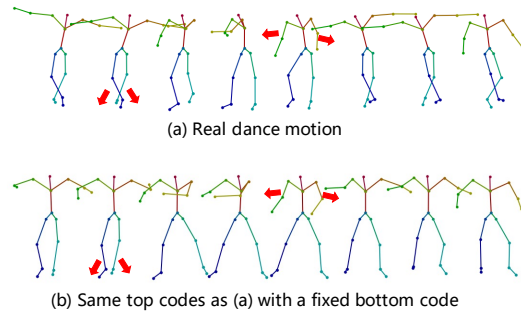


Figure 6. (a) A real dance motion sequence. (b) Replace bottom code of (a) with a fixed value. Red arrows represent motion trends (dance movements). While the motion of (b) is constrained due to the fixed bottom code, it still maintains the same dance movements as (a), e.g., opening legs in the second column and lifting hands horizontally in the fifth column.

The Interpretability of Top Code. As shown in Fig.6(a), we first select a segment of dance motion sequence and display it in the time dimension. Next, we replace the bottom code of this dance segment with a fixed value, as illustrated in Fig.6(b). Since the bottom code is replaced with a fixed value, the motion in Fig.6(b) is constrained within a certain range. However, from the temporal perspective, the motion trends (dance movements) of the two are consistent, e.g., opening legs in the second column and lifting hands horizontally in the fifth column (red arrows represent motion

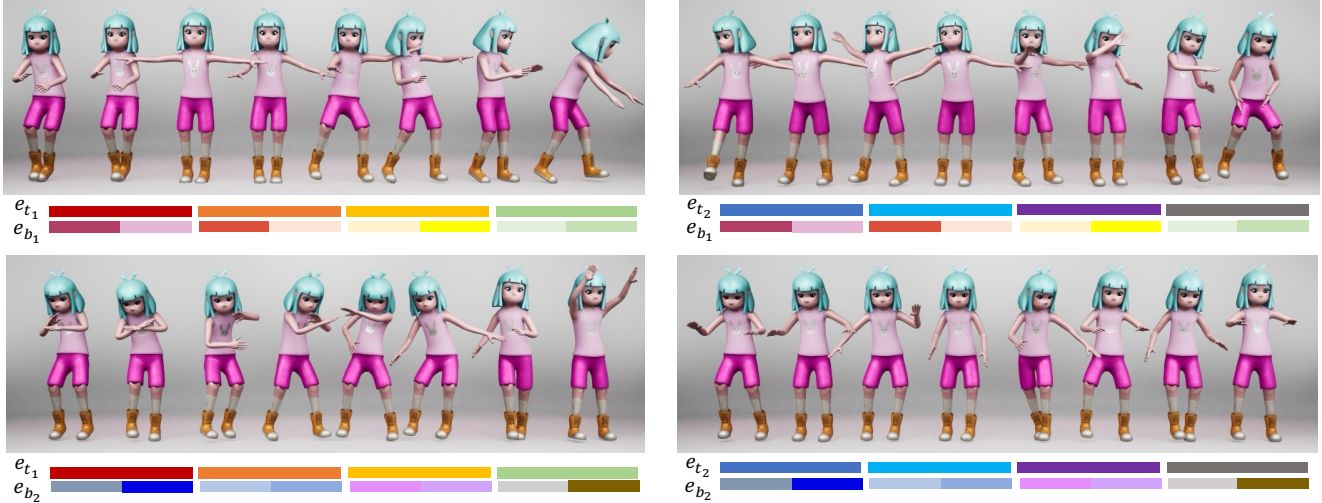


Figure 7. Results of transferring bottom code and top code. e_{t_1} and e_{t_2} represent two sets of top codes, e_{b_1} and e_{b_2} represent two sets of bottom codes. By modifying the top code (within the same row), the dance poses are retained, but the movements of the motion are altered. By modifying the bottom code (within the same column), the specific dance poses change, but the motion movements are preserved.



Figure 8. Generated dance can be edited by inserting, deleting, replacing, or modifying the relative order of latent codes.

trends), which demonstrates that the top code can characterize dance movements. Please refer to the supplementary materials for more visual results.

4.4. Applications

Through the above verification of the interpretability of top code and bottom code, we’ve confirmed that the bottom code has the ability to represent dance poses, while the top code can signify dance movements. Using a hierarchical VQ-VAE structure, we have successfully decoupled dance pose and dance movement, enabling diverse applications. For example, by transferring different top codes, we can control the style, speed, and motion trends of the dance, as illustrated in Fig.7, e_{t_1} and e_{t_2} represent two sets of top codes, e_{b_1} and e_{b_2} represent two sets of bottom codes. Different colors indicate different latent codes. By modifying the top code (within the same row), the dance poses are retained, but the speed and movements of the motion are altered. By modifying the bottom code (within the same column), the specific dance poses change, but the motion

trends and dance movements are preserved. Furthermore, we can use this capability to achieve choreography editing. As illustrated in Fig.8, since the latent code corresponds to a dance phrase in a specific time segment, we can edit the generated dance by inserting, deleting, replacing, or modifying the relative order of latent codes.

5. Limitations and Future Works

Generating long-term and temporally coherent dance sequences remains a challenge. While our method can generate dance sequences of any length by applying temporal constraints to batches [38], there is still a need to explore a way to model the global consistency like [2], reflecting the concept of dance sections. In addition, the efficiency of diffusion-based methods is relatively low, preventing real-time generation. Consistency models[26, 34] may be a potential improvement to accelerate the generation process.

6. Conclusions

Our method draws inspiration from the domain of choreography and introduces a two-stage generative framework named DanceMeld. In the decouple stage, a hierarchical VQ-VAE is trained to obtain the bottom code and top code, representing dance pose and dance movement. In the generation stage, a diffusion model serves as a prior for modeling and sampling latent codes. We conduct several experiments to demonstrate the interpretability of bottom code and top code, demonstrating applications such as dance style transfer and dance editing. Validation on the AIST++ dataset reveals state-of-the-art performance, supported by both qualitative and quantitative results.

References

- [1] Simon Alexanderson, Rajmund Nagy, Jonas Beskow, and Gustav Eje Henter. Listen, denoise, action! audio-driven motion synthesis with diffusion models. *ACM Transactions on Graphics (TOG)*, 42(4):1–20, 2023. 2
- [2] Andreas Aristidou, Anastasios Yiannakidis, Kfir Aberman, Daniel Cohen-Or, Ariel Shamir, and Yiorgos Chrysanthou. Rhythm is a dancer: Music-driven motion synthesis with global structure. *IEEE Transactions on Visualization and Computer Graphics*, 2022. 2, 8
- [3] Lynne Anne Blom and L Tarin Chaplin. *The intimate act of choreography*. University of Pittsburgh Pre, 1982. 2
- [4] Kang Chen, Zhipeng Tan, Jin Lei, Song-Hai Zhang, Yuan-Chen Guo, Weidong Zhang, and Shi-Min Hu. Choreomaster: choreography-oriented music-driven dance synthesis. *ACM Transactions on Graphics (TOG)*, 40(4):1–13, 2021. 2
- [5] Xin Chen, Biao Jiang, Wen Liu, Zilong Huang, Bin Fu, Tao Chen, and Gang Yu. Executing your commands via motion diffusion in latent space. In *Proceedings of the IEEE/CVF Conference on Computer Vision and Pattern Recognition*, pages 18000–18010, 2023. 3
- [6] Rishabh Dabral, Muhammad Hamza Mughal, Vladislav Golyanik, and Christian Theobalt. Mofusion: A framework for denoising-diffusion-based motion synthesis. In *Proceedings of the IEEE/CVF Conference on Computer Vision and Pattern Recognition*, pages 9760–9770, 2023. 2, 3
- [7] Jeffrey De Fauw, Sander Dieleman, and Karen Simonyan. Hierarchical autoregressive image models with auxiliary decoders. *arXiv preprint arXiv:1903.04933*, 2019. 3
- [8] Prafulla Dhariwal, Heewoo Jun, Christine Payne, Jong Wook Kim, Alec Radford, and Ilya Sutskever. Jukebox: A generative model for music. *arXiv preprint arXiv:2005.00341*, 2020. 3, 4
- [9] Sander Dieleman, Aaron van den Oord, and Karen Simonyan. The challenge of realistic music generation: modelling raw audio at scale. *Advances in neural information processing systems*, 31, 2018. 3
- [10] Jibin Gao, Junfu Pu, Honglun Zhang, Ying Shan, and Wei-Shi Zheng. Pc-dance: Posture-controllable music-driven dance synthesis. In *Proceedings of the 30th ACM International Conference on Multimedia*, pages 1261–1269, 2022. 2
- [11] Kehong Gong, Dongze Lian, Heng Chang, Chuan Guo, Zihang Jiang, Xinxin Zuo, Michael Bi Mi, and Xinchao Wang. Tm2d: Bimodality driven 3d dance generation via music-text integration. In *Proceedings of the IEEE/CVF International Conference on Computer Vision*, pages 9942–9952, 2023. 3
- [12] Shuyang Gu, Dong Chen, Jianmin Bao, Fang Wen, Bo Zhang, Dongdong Chen, Lu Yuan, and Baining Guo. Vector quantized diffusion model for text-to-image synthesis. In *Proceedings of the IEEE/CVF Conference on Computer Vision and Pattern Recognition*, pages 10696–10706, 2022. 5
- [13] Fangzhou Hong, Mingyuan Zhang, Liang Pan, Zhongang Cai, Lei Yang, and Ziwei Liu. Avatarclip: Zero-shot text-driven generation and animation of 3d avatars. *arXiv preprint arXiv:2205.08535*, 2022. 3
- [14] Ruozhi Huang, Huang Hu, Wei Wu, Kei Sawada, Mi Zhang, and Daxin Jiang. Dance revolution: Long-term dance generation with music via curriculum learning. *arXiv preprint arXiv:2006.06119*, 2020. 2
- [15] Tero Karras, Samuli Laine, and Timo Aila. A style-based generator architecture for generative adversarial networks. In *Proceedings of the IEEE/CVF conference on computer vision and pattern recognition*, pages 4401–4410, 2019. 3
- [16] Tero Karras, Samuli Laine, Miika Aittala, Janne Hellsten, Jaakko Lehtinen, and Timo Aila. Analyzing and improving the image quality of stylegan. In *Proceedings of the IEEE/CVF conference on computer vision and pattern recognition*, pages 8110–8119, 2020. 3
- [17] Jinwoo Kim, Heeseok Oh, Seongjean Kim, Hoseok Tong, and Sanghoon Lee. A brand new dance partner: Music-conditioned pluralistic dancing controlled by multiple dance genres. In *Proceedings of the IEEE/CVF Conference on Computer Vision and Pattern Recognition*, pages 3490–3500, 2022. 2
- [18] Jihoon Kim, Jiseob Kim, and Sungjoon Choi. Flame: Free-form language-based motion synthesis & editing. In *Proceedings of the AAAI Conference on Artificial Intelligence*, pages 8255–8263, 2023. 3
- [19] Diederik P Kingma and Jimmy Ba. Adam: A method for stochastic optimization. *arXiv preprint arXiv:1412.6980*, 2014. 5
- [20] Hsin-Ying Lee, Xiaodong Yang, Ming-Yu Liu, Ting-Chun Wang, Yu-Ding Lu, Ming-Hsuan Yang, and Jan Kautz. Dancing to music. *Advances in neural information processing systems*, 32, 2019. 2
- [21] Taeryung Lee, Gyeongsik Moon, and Kyoung Mu Lee. Multiact: Long-term 3d human motion generation from multiple action labels. In *Proceedings of the AAAI Conference on Artificial Intelligence*, pages 1231–1239, 2023. 3
- [22] Buyu Li, Yongchi Zhao, Shi Zhelun, and Lu Sheng. Danceformer: Music conditioned 3d dance generation with parametric motion transformer. In *Proceedings of the AAAI Conference on Artificial Intelligence*, pages 1272–1279, 2022. 2
- [23] Ruilong Li, Shan Yang, David A Ross, and Angjoo Kanazawa. Ai choreographer: Music conditioned 3d dance generation with aist++. In *Proceedings of the IEEE/CVF International Conference on Computer Vision*, pages 13401–13412, 2021. 2, 5, 6
- [24] Ronghui Li, Junfan Zhao, Yachao Zhang, Mingyang Su, Zeping Ren, Han Zhang, Yansong Tang, and Xiu Li. Finedance: A fine-grained choreography dataset for 3d full body dance generation. In *Proceedings of the IEEE/CVF International Conference on Computer Vision*, pages 10234–10243, 2023. 2
- [25] Matthew Loper, Naureen Mahmood, Javier Romero, Gerard Pons-Moll, and Michael J Black. Smpl: A skinned multi-person linear model. In *Seminal Graphics Papers: Pushing the Boundaries, Volume 2*, pages 851–866. 2023. 4
- [26] Simian Luo, Yiqin Tan, Longbo Huang, Jian Li, and Hang Zhao. Latent consistency models: Synthesizing high-resolution images with few-step inference, 2023. 8

- [27] Jianxin Ma, Shuai Bai, and Chang Zhou. Pretrained diffusion models for unified human motion synthesis. *arXiv preprint arXiv:2212.02837*, 2022. 3
- [28] Sandra Cerny Minton. *Choreography: a basic approach using improvisation*. Human Kinetics, 2017. 2
- [29] Junfu Pu and Ying Shan. Music-driven dance regeneration with controllable key pose constraints. *arXiv preprint arXiv:2207.03682*, 2022. 2
- [30] Alec Radford, Jong Wook Kim, Chris Hallacy, Aditya Ramesh, Gabriel Goh, Sandhini Agarwal, Girish Sastry, Amanda Askell, Pamela Mishkin, Jack Clark, et al. Learning transferable visual models from natural language supervision. In *International conference on machine learning*, pages 8748–8763. PMLR, 2021. 3
- [31] Ali Razavi, Aaron Van den Oord, and Oriol Vinyals. Generating diverse high-fidelity images with vq-vae-2. *Advances in neural information processing systems*, 32, 2019. 2, 3
- [32] Yonatan Shafir, Guy Tevet, Roy Kapon, and Amit H Bermano. Human motion diffusion as a generative prior. *arXiv preprint arXiv:2303.01418*, 2023. 3
- [33] Li Siyao, Weijiang Yu, Tianpei Gu, Chunze Lin, Quan Wang, Chen Qian, Chen Change Loy, and Ziwei Liu. Bailando: 3d dance generation by actor-critic gpt with choreographic memory. In *Proceedings of the IEEE/CVF Conference on Computer Vision and Pattern Recognition*, pages 11050–11059, 2022. 2, 3, 6
- [34] Yang Song, Prafulla Dhariwal, Mark Chen, and Ilya Sutskever. Consistency models. 2023. 8
- [35] Jiangxin Sun, Chunyu Wang, Huang Hu, Hanjiang Lai, Zhi Jin, and Jian-Fang Hu. You never stop dancing: Non-freezing dance generation via bank-constrained manifold projection. *Advances in Neural Information Processing Systems*, 35:9995–10007, 2022. 2
- [36] Guy Tevet, Brian Gordon, Amir Hertz, Amit H Bermano, and Daniel Cohen-Or. Motionclip: Exposing human motion generation to clip space. In *European Conference on Computer Vision*, pages 358–374. Springer, 2022. 3
- [37] Guy Tevet, Sigal Raab, Brian Gordon, Yonatan Shafir, Daniel Cohen-Or, and Amit H Bermano. Human motion diffusion model. *arXiv preprint arXiv:2209.14916*, 2022. 3
- [38] Jonathan Tseng, Rodrigo Castellon, and Karen Liu. Edge: Editable dance generation from music. In *Proceedings of the IEEE/CVF Conference on Computer Vision and Pattern Recognition*, pages 448–458, 2023. 2, 3, 6, 8
- [39] Aaron Van Den Oord, Oriol Vinyals, et al. Neural discrete representation learning. *Advances in neural information processing systems*, 30, 2017. 2, 3, 4
- [40] Xingyu Xie, Pan Zhou, Huan Li, Zhouchen Lin, and Shuicheng Yan. Adan: Adaptive nesterov momentum algorithm for faster optimizing deep models. *arXiv preprint arXiv:2208.06677*, 2022. 6
- [41] Zijie Ye, Haozhe Wu, Jia Jia, Yaohua Bu, Wei Chen, Fanbo Meng, and Yanfeng Wang. Choreonet: Towards music to dance synthesis with choreographic action unit. In *Proceedings of the 28th ACM International Conference on Multimedia*, pages 744–752, 2020. 2
- [42] Wenjie Yin, Hang Yin, Kim Baraka, Danica Kragic, and Mårten Björkman. Dance style transfer with cross-modal transformer. In *Proceedings of the IEEE/CVF Winter Conference on Applications of Computer Vision*, pages 5058–5067, 2023. 2
- [43] Mingyuan Zhang, Zhongang Cai, Liang Pan, Fangzhou Hong, Xinying Guo, Lei Yang, and Ziwei Liu. Motiondiffuse: Text-driven human motion generation with diffusion model. *arXiv preprint arXiv:2208.15001*, 2022. 3
- [44] Mingyuan Zhang, Xinying Guo, Liang Pan, Zhongang Cai, Fangzhou Hong, Huirong Li, Lei Yang, and Ziwei Liu. Remodiffuse: Retrieval-augmented motion diffusion model. *arXiv preprint arXiv:2304.01116*, 2023.
- [45] Mengyi Zhao, Mengyuan Liu, Bin Ren, Shuling Dai, and Nicu Sebe. Modiff: Action-conditioned 3d motion generation with denoising diffusion probabilistic models. *arXiv preprint arXiv:2301.03949*, 2023. 3
- [46] Zhuoran Zhao, Jinbin Bai, Delong Chen, Debang Wang, and Yubo Pan. Taming diffusion models for music-driven conducting motion generation. *arXiv preprint arXiv:2306.10065*, 2023. 3
- [47] Zixiang Zhou and Baoyuan Wang. Ude: A unified driving engine for human motion generation. In *Proceedings of the IEEE/CVF Conference on Computer Vision and Pattern Recognition*, pages 5632–5641, 2023. 3
- [48] Wenlin Zhuang, Congyi Wang, Jinxiang Chai, Yangang Wang, Ming Shao, and Siyu Xia. Music2dance: Dancenet for music-driven dance generation. *ACM Transactions on Multimedia Computing, Communications, and Applications (TOMM)*, 18(2):1–21, 2022. 2